# Rigid-Backbone Polymers. Dielectric Relaxation of Isotropic and Lyotropic Solutions of Poly(*n*-hexyl isocyanate)

**Jozef K. Moscicki† and Graham Williams***

*Edward Davies Chemical Laboratories, University College of Wales, Aberystwyth, Dyfed SY23 1NE, United Kingdom*

**Shaul M. Aharoni**

*Allied Chemical Corporation, Morristown, New Jersey 07960.* *Received September 8, 1981*

ABSTRACT: The dielectric behavior of a sample of poly(*n*-hexyl isocyanate) in toluene has been studied over a range of concentration and temperature to include the isotropic, biphasic, and anisotropic phases. It is shown that as the concentration $c$ of polymer is raised in the isotropic phase, the relaxation magnitude $\Delta\epsilon$ and relaxation time $\langle\tau\rangle = \{2\pi f_m\}^{-1}$ steadily increase, but above a critical concentration, $\Delta\epsilon$ and $\langle\tau\rangle$ fall with increased concentration in a fairly narrow range of $c$, which corresponds to the biphasic range, and then take on values characteristic of the anisotropic phase. It is shown that the biphasic range may be traversed by varying concentration and/or temperature and that the magnitude and location of the loss process provide a very sensitive means for studying the structure and dynamics of the phases. The dielectric behavior is interpreted by using the Flory theory for the phase behavior of rodlike particles in solution, as developed by Moscicki and Williams for the special case of a Gaussian distribution of molecular weight, together with theories due to Warchol and Vaughan and to Wang and Pecora for motions of chains constrained to a virtual cone prescribed by the neighboring molecules in the anisotropic phase.

## Introduction

Aharoni and co-workers[1-8] have recently shown that certain poly(alkyl isocyanates) exhibit lyotropic-nematic liquid-crystal behavior in concentrated solution. The formation of a mesophase, the phase equilibrium between isotropic and anisotropic phases in a biphasic system, as observed by Aharoni and Walsh,[2,3] and the partial fractionation of the polymer between these two phases were essentially in accord with the theoretical predictions of Flory and co-workers[9-14] for the phase behavior of polydisperse rodlike molecules in solution at high concentration. The observations of nematic liquid-crystal phases arising for rodlike molecules in solution is not unique to the poly(alkyl isocyanates). The $\alpha$-helical polypeptides[15-20] and certain aromatic polyamides[21-24] also exhibit liquid-crystalline behavior in suitable solvents due, presumably, to the rodlike (or stiff) properties of their chains.

Studies of the structure and dynamics of such systems may be made by such techniques as dielectric relaxation, Kerr effect relaxation, quasi-elastic polarized and depolarized light scattering, quasi-elastic neutron scattering, and $^1H$ and $^{13}C$ NMR relaxation. The dielectric technique is particularly useful since a wide range of frequency is readily studied, and information is obtained on the $P_1$ auto- and cross-correlation functions for the angular motions of the molecules. (See, for example, ref 25 and 26 and references therein for information on the time-correlation functions which are involved in dielectric relaxation and related techniques.) While dielectric studies are extremely difficult for certain helical polypeptides and aromatic polyamides due to the highly polar or ionic solvents involved,[15-24] such studies for poly(alkyl isocyanates) are more readily achieved since they are soluble to high concentration in solvents of low polarity such as benzene, toluene, and chloroform. Thus studies of the dielectric behavior of poly(alkyl isocyanates) in such solvents, covering the isotropic and lyotropic-nematic ranges, serve as model studies which may give information that is of value for an understanding of the phase behavior, structure, and dynamics of polydisperse rodlike molecules in solution in general. Earlier studies have been made of the dielectric[27-33] and dynamic Kerr effect[32-34] behavior of isotropic solutions of poly(*n*-alkyl isocyanates) in solution, with the pendant group ranging from *n*-butyl to *n*-octyl. We have reported[35] preliminary dielectric data for a sample of poly(*n*-hexyl isocyanate) in toluene covering the isotropic and lyotropic ranges and have shown that the magnitude of the dielectric relaxation curve, $\Delta\epsilon$, and the average dielectric relaxation time, $\langle\tau\rangle$, both decrease on going from the isotropic to lyotropic-nematic states. We conducted a more extensive dielectric study[36] of a copolymer of *n*-butyl isocyanate and *n*-nonyl isocyanate in toluene in which the earlier results[35] were confirmed and interpretations of the motion in the isotropic and lyotropic-nematic states were made in terms of small-step rotational diffusion with a $4\pi$ solid angle and within a "virtual cone" (prescribed by a local director), respectively. We applied the theories of Warchol and Vaughan[37] and Wang and Pecora[38] for small-step diffusion restricted to a cone for the limited motions in the nematic phase, and it was shown that these theories predict that as the extent of angular motion is increasingly limited in solid angle so $\Delta\epsilon$ and $\langle\tau\rangle$ decrease—as was observed experimentally.[35,36]

The present paper reports extensive dielectric data for a sample of poly(*n*-hexyl isocyanate) in toluene covering the ranges 4.9–40.4% (w/w) concentration of polymer, 2–$10^5$ Hz, and 253–313 K and thus represents the most comprehensive study, to date, of the dielectric relaxation behavior of a rodlike polymer in solution.

## Experimental Section

The sample of poly(*n*-hexyl isocyanate) (PHIC) was made in a 50:50 mixture of dimethylformamide and toluene. It had an intrinsic viscosity of 2.15 dL g$^{-1}$ in toluene and 2.14 dL g$^{-1}$ in chloroform. Its weight-average molecular weight was determined by a Zimm plot from light scattering measurements in tetrachloroethane to be 76 000 ± 2000. The number-average molecular weight was determined in a Mechrolab membrane osometer, using chloroform as solvent, giving a value 55 000 ± 2000. Thus $M_w/M_n = 1.38$. These measurements were made at ambient temperature (296 K). The value of $M_w$ obtained by us is the same as that expected from the relationship of Berger and Tidswell.[39] Eight solutions, 4.9, 10.0, 14.8, 21.4, 25.0, 30.6, 35.3, and 40.4% polymer (w/w) in toluene, covering the isotropic and lyotropic-nematic phases at room temperature, were investigated. The toluene was of AR grade and was dried over zeolite before use. Solutions were made by gently shaking polymer/solvent mixtures for many hours,

† Permanent address: Institute of Physics, Jagellonian University, 30-59 Krakow, Poland.

0024-9297/82/2215-0642$01.25/0 

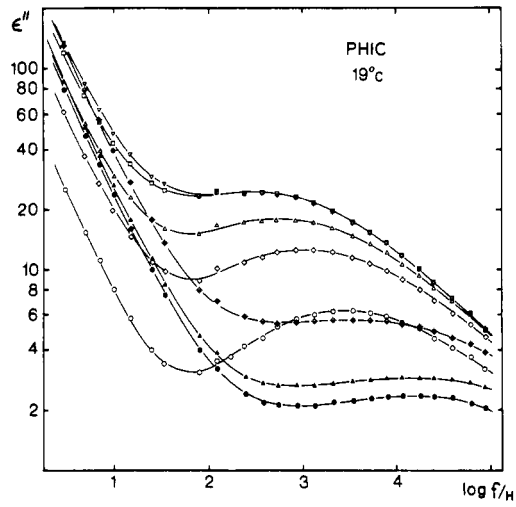


**Figure 1.** $\epsilon''$ against log ($f$/Hz) for PHIC in toluene at 292.2 K: (○) 4.9%; (◇) 10.0%; (△) 14.8%; (□) 21.4%; (▽) 25.0%; (⊕) 30.6%; (▲) 35.3%; (●) 40.4% polymer (w/w).

followed by centrifugation in order to deposit particulate matter and to eliminate air bubbles. In order to avoid problems with the evaporation of solvent at the higher temperatures, a specially designed cell[36] was employed for all measurements. The dielectric measurements were made by using a three-terminal arrangement of the cell and employed a Sullivan C306D transformer bridge (60–$10^5$ Hz) and a Scheiber bridge ($10^{-2}$–$10^2$ Hz). Agreement within 1% was obtained for the components of the complex permittivity ($\epsilon = \epsilon' - i\epsilon''$) when measured by both bridges in their range of overlap. All solutions exhibited marked conductivity effects at low frequencies. Figure 1 shows the dielectric loss factor $\epsilon''$ as a function of frequency for PHIC/toluene solutions at 292.2 K. Note the logarithmic scale in $\epsilon''$ in the figure and the large magnitude of $\epsilon''$ reached at the lowest frequencies. Such data were analyzed as being a sum of dc and relaxation conductivity processes, so

$$\epsilon''(f) = \epsilon''_{dc} + \epsilon''_r = \frac{1.8 \times 10^{12}\sigma}{f} + \epsilon''_r(f) \quad (1)$$

where $\sigma$ and $f$ are specific conductivity ($\Omega^{-1}$ cm$^{-1}$) and frequency (Hz), respectively. A dc conductivity may lead to an electrode polarization and hence to a difference between the observed ($\epsilon'$) and "intrinsic" ($\epsilon'_r$) permittivites of the material. This has the form[40]

$$\epsilon'_r = \epsilon' - \delta/f^2 \quad (2)$$

We may expand $\epsilon'_r$ and $\epsilon''_r$ as power series in $f^n$ and obtain

$$\epsilon''f = \sigma + b_1f^2 + b_2f^3 + \ldots \quad (3a)$$

$$\epsilon'f^2 = \delta + \epsilon_\infty f^2 + a_1f^3 + a_2f^4 + \ldots \quad (3b)$$

where $\epsilon_\infty$ is the limiting high-frequency permittivity. Using eq 3, we have fitted the low-frequency data (with respect to the loss maxima) by a least-squares procedure, allowing $\delta$ and $\sigma$ to be determined and hence allowing $\epsilon''_r$ and $\epsilon'_r$ to be evaluated at each frequency by eq 1 and 2, respectively.

## Results

Figures 2 and 3 show a representative portion of our data for $\epsilon'_r$ and $\epsilon''_r$ for PHIC in toluene at different polymer concentrations ($c$ in percent (w/w)) and at 292.2 K. Such curves contain information on the variation of (i) the magnitude $\Delta\epsilon = \epsilon_{r0} - \epsilon_\infty = \int \epsilon''\, d \ln f$, (ii) the frequency location $f_m = \{2\pi\langle\tau\rangle\}^{-1}$, where $\langle\tau\rangle$ is an average relaxation time, and (iii) the shape of the loss process with polymer concentration.

Figure 4 shows log ($f_m$/Hz), log ($\sigma$/($\Omega^{-1}$ cm$^{-1}$)), the static permittivity $\epsilon_{r0}$, and the values of the maximum loss factor $\epsilon''_m$ plotted against $c$ for PHIC at 292.2 K. These quantities were obtained from the data of Figures 1–3. Also

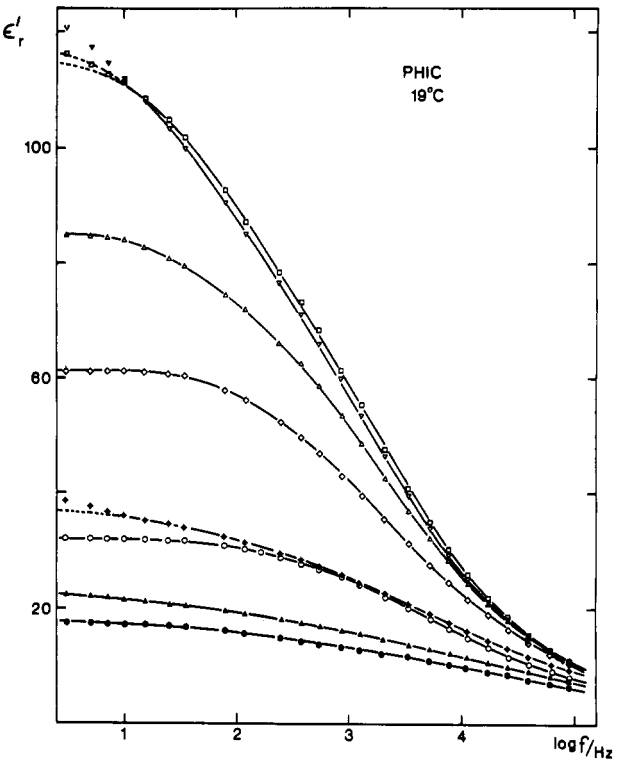


**Figure 2.** $\epsilon'$ against log ($f$/Hz) for PHIC in toluene at 292.2 K: (○) 4.9%; (◇) 10.0%; (△) 14.8%; (□) 21.4%; (▽) 25.0%; (⊕) 30.6%; (▲) 35.3%; (●) 40.4% polymer (w/w). The continuous curves correspond to $\epsilon'_r$.

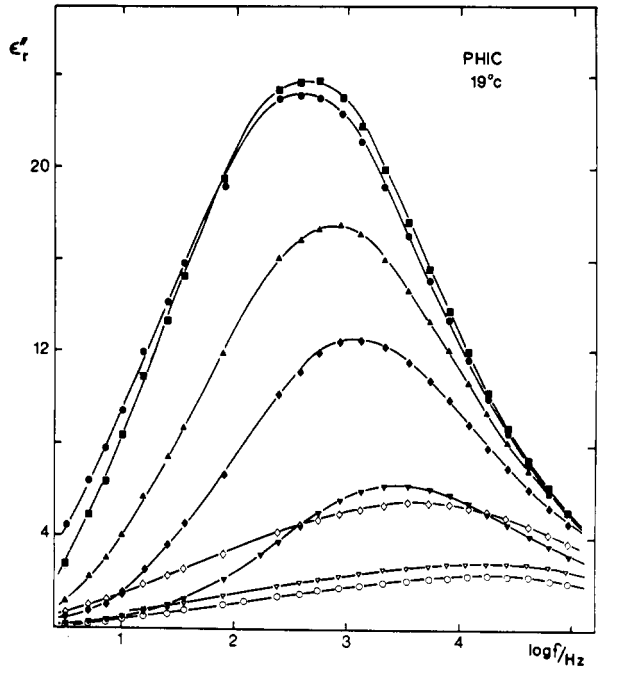


**Figure 3.** $\epsilon''_r$ against log ($f$/Hz) for PHIC in toluene at 292.2 K: (▼) 4.9%; (♦) 10.0%; (▲) 14.8%; (■) 21.4%; (●) 25.0%; (◇) 30.6%; (▽) 35.3%; (○) 40.4% polymer (w/w).

shown for comparison purposes are our data[36] for a copolymer of $n$-butyl isocyanate and $n$-nonyl isocyanate in toluene. From Figures 2–4 we have the following observations for PHIC in toluene.

For the range $0 < c < 15\%$, both $\epsilon_{r0}$ and $\epsilon''_m$ increase linearly with $c$. Further increase in $c$ leads to an increasing downward deviation of these quantities from the linear relation until $c = 22\%$, beyond which both quantities exhibit a dramatic fall. A consideration of log $f_m$ shows that the values decrease approximately linearly with increasing

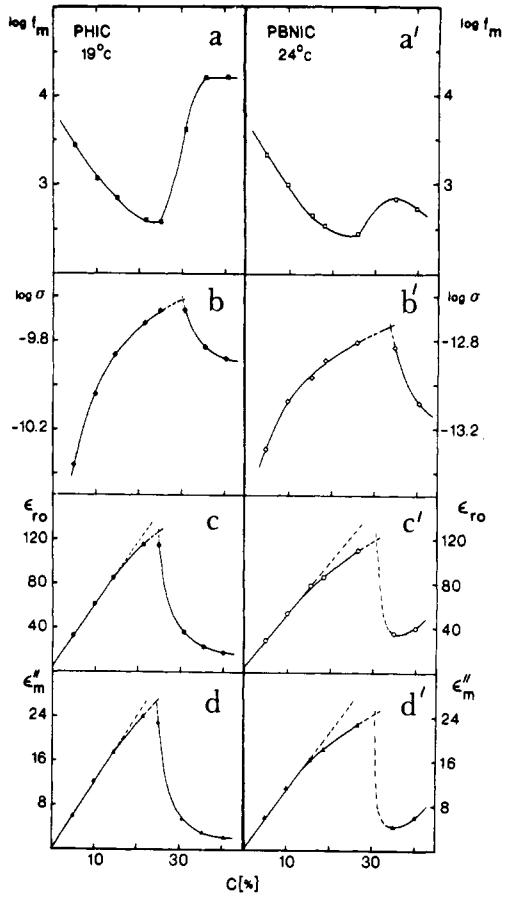


**Figure 4.** (a) log ($f_m$/Hz), (b) log ($\sigma$/($\Omega^{-1}$ cm$^{-1}$)), (c) $\epsilon_{r0}$, and (d) $\epsilon''_m$ as a function of polymer concentration (% (w/w)) for PHIC–toluene solutions at 292.2 K. Also shown as (a'), (b'), (c'), and (d') are the corresponding plots for a copolymer of *n*-butyl isocyanate and *n*-nonyl isocyanate in toluene as obtained from earlier studies.[36]

*c* to $c \simeq 15\%$ and then show a gradually decreasing slope until 22% is reached, after which the values show a very marked increase, reaching an apparent plateau beyond $c \simeq 35\%$. Up to about 15% polymer the solutions are isotropic but at the higher concentrations they form a lyotropic-nematic mesophase, as evidenced by their turbidity and by the observations of characteristic structures in the optical polarizing microscope. Figure 5 shows the Cole–Cole (or Argand) diagram for two compositions, one below and one above the break point for $\epsilon_{r0}$ (and $\epsilon''_m$) in Figure 4. Figure 5, taken together with Figure 3, shows that the loss curves in the isotropic range are asymmetrical in the Cole–Davidson sense, with a half-width near 2.6, in units of log ($f$/Hz), but in the lyotropic-nematic range the loss curves are far broader, with half-widths near 4.8, and are symmetrical in the Cole–Cole sense.

We have studied the effect of varying the temperature on the dielectric behavior of isotropic and lyotropic-nematic solutions. For $c < 15\%$, increase in temperature leads to a marked decrease in $\Delta\epsilon$, $\epsilon''_m$, and $\langle\tau\rangle$, in accord with our earlier observations for poly(*n*-butyl isocyanate) and poly(*n*-octyl isocyanate) in carbon tetrachloride.[32] Figures 6–8 show the behavior of $\epsilon''_r(f)$ at $c$ = 25.0, 30.7, and 35.3% polymer at different temperatures. For $c$ = 25.0%, inspection of Figures 4 and 6 suggest that at 292.2 K the solution is beginning to deviate from a wholly isotropic solution. Figure 6 shows that an increase in temperature to 313.2 K gives a *decrease* in $\epsilon''_m$ and a shift of log $f_m$ to higher values, in agreement with the behavior for an isotropic solution. However, decrease in temperature to 274.2 K leads to a remarkable decrease in $\epsilon''_m$ and only a very slight shift of log $f_m$ to lower values. Thus the system departs dramatically from isotropic behavior for $T < 292.2$ K. In Figure 7 at 292.2 K the system is in the lyotropic-nematic range. Further decreases in temperature to 274.2 and 253.2 K lead first to a decrease in $\epsilon''_m$ accompanied by a slight shift to higher values of log $f_m$ (i.e., comparing 292.2 and 274.2 K) and then to a slight increase in $\epsilon''_m$ accompanied by a marked decrease in log $f_m$ (i.e., comparing 274.2 and 253.2 K). Thus decrease of temperature in the range 292.2–253.2 K consolidates the formation of the lyotropic-nematic phase. Increase in temperature from 292.2 to 313.2 K leads to a marked increase in $\epsilon''_m$ and a *decrease*[46] in log $f_m$, and the directions of these variations are maintained on further increase to 333.2 K. Clearly, the loss curves in this range show that the lyotropic-nematic material is being transformed gradually, with increased temperature, into the isotropic phase with its attendant larger mean-square dipole moment $\langle\mu^2\rangle$. Similar behavior is observed in Figure 8. Starting at 253.2 K, increase of temperature initially leads to an increase in $\epsilon''_m$ and log $f_m$, as expected in the lyotropic-nematic range, but for temperatures exceeding 292.2 K, there is a marked increase in $\epsilon''_m$ and a *decrease* in log $f_m$, showing that the lyotropic-nematic material is gradually transforming into the isotropic phase with increase in temperature.

In order to obtain an overall impression of the variations of the dielectric behavior of PHIC with concentration and temperature, we have processed our $\epsilon''_m(c,T)$ and log $f_m(c,T)$ data to yield the contour diagrams shown in Figures 9 and 10. The lines defining the surface of $\epsilon''_m$ and low

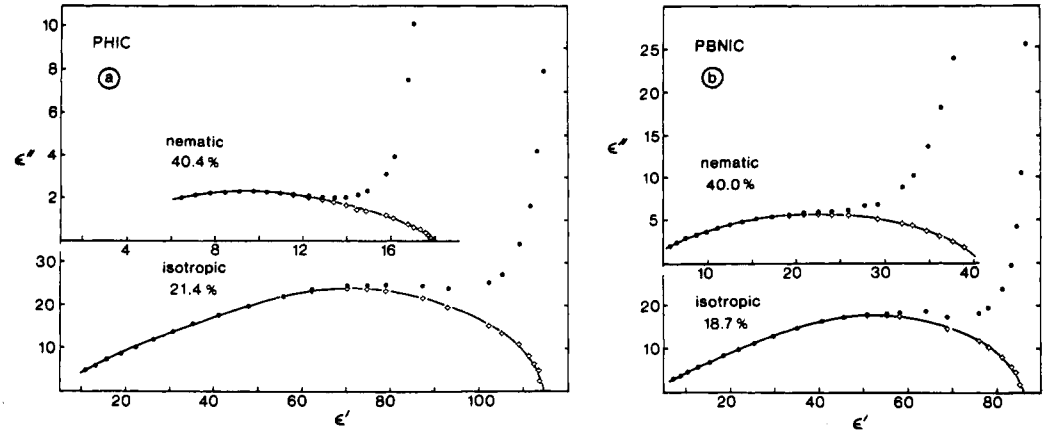


**Figure 5.** Argand diagram of $\epsilon''$ against $\epsilon'$ for (a) $c$ = 40.4% (w/w) and $c$ = 21.4% (w/w) solutions of PHIC in toluene at 292.2 K and for (b) $c$ = 40.0% (w/w) and $c$ = 18.7% (w/w) solutions of PBNIC in toluene at 292.2 K.

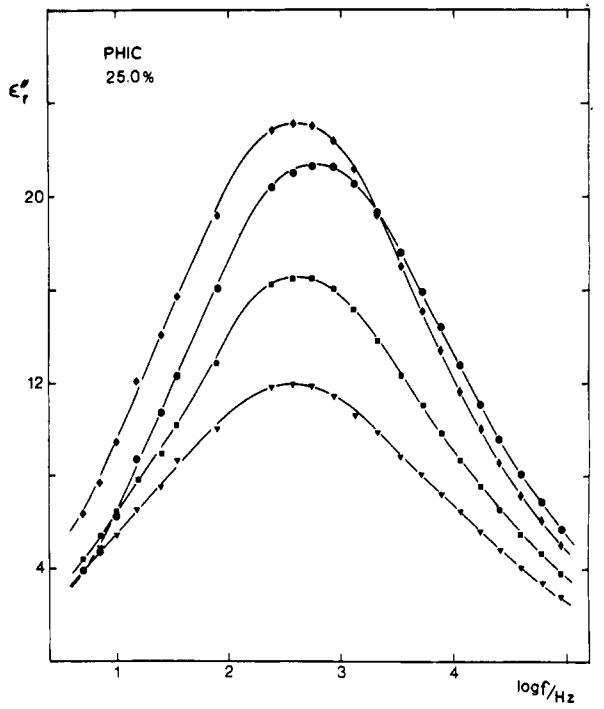


**Figure 6.** $\epsilon''_r$ against log ($f$/Hz) for a 25.0% PHIC–toluene solution: (▼) 253.2 K; (■) 274.2 K; (♦) 292.2 K; (●) 313.2 K.

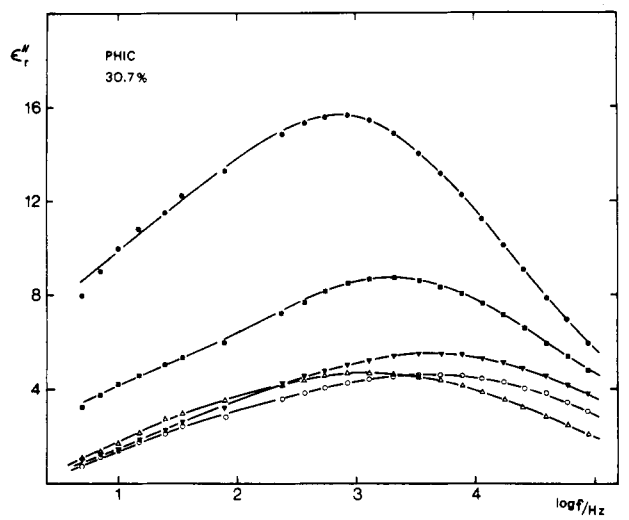


**Figure 7.** $\epsilon''_r$ against log ($f$/Hz) for a 30.7% PHIC–toluene solution: (△) 253.2 K; (○) 274.2 K; (▼) 292.2 K; (■) 313.2 K; (●) 333.2 K.

$f_m$ are constructed such that they would lie diagonally across the surface if the surface was parallel with the basal plane ($c$, $T$). Figure 9 shows that $\epsilon''_m$, at constant $T$, increases with $c$ in the isotropic range, goes through a maximum, and decreases over a wide range of $c$. As $T$ is increased the value of $\epsilon''_m$ at the peak decreases and the concentration corresponding to this maximum increases; i.e., the higher the temperature, the higher the concentration for the formation of the lyotropic-nematic material. In Figure 10 we see that log $f_m$ initially decreases with increasing $c$ at constant $T$ for the isotropic material, goes through a minimum, and then increases sharply with further increase in $c$. As the temperature is raised, the minimum becomes more shallow and its location moves to higher values of $c$. Figures 9 and 10 are complementary and indicate that the transformation from isotropic to lyotropic-nematic material occurs over a range of $c$ for $c$ greater than a critical value $c^*$, whose value increases with increasing temperature, and that the transformation becomes more diffuse as the temperature is increased.

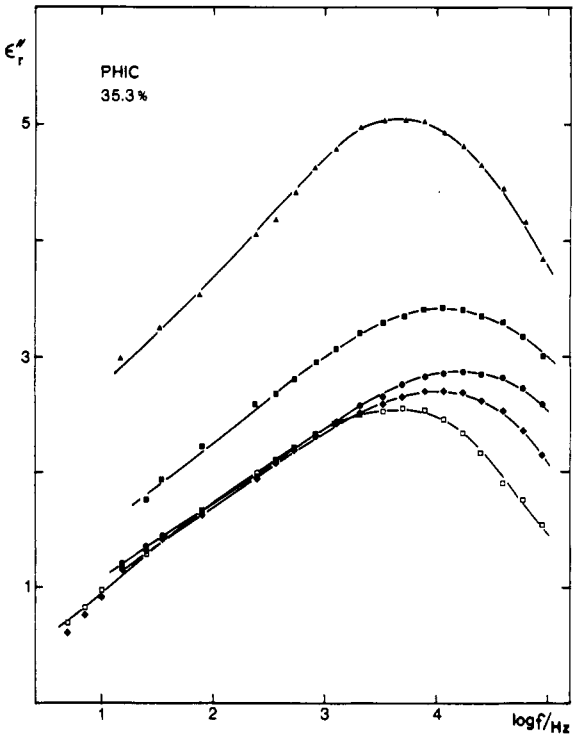


**Figure 8.** $\epsilon''_r$ against log ($f$/Hz) for a 35.3% PHIC–toluene solution: (□) 253 K; (◊) 274.2 K; (●) 292.2 K; (■) 313.2 K; (▲) 333.2 K.

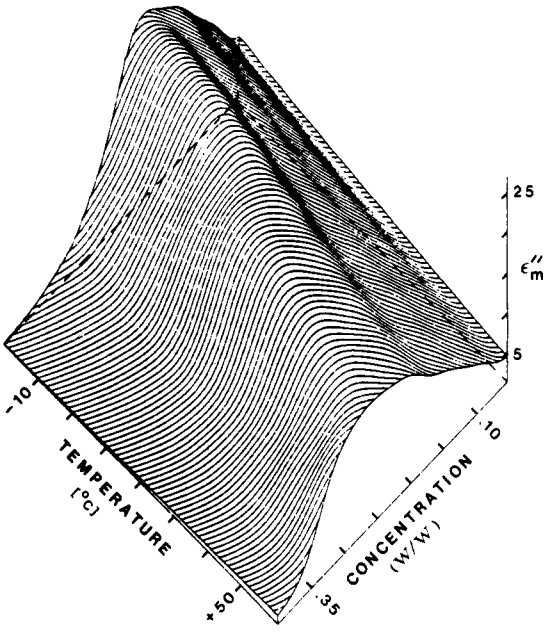


**Figure 9.** $\epsilon''_m$ as a function of $c$ and $T$/°C for PHIC in toluene.

## Discussion

Since we have studied both equilibrium and dynamic aspects of the dielectric behavior of both the isotropic and lyotropic-nematic phases for PHIC–toluene solutions, it is essential to briefly indicate the relations between the macroscopic dielectric quantities and the molecular dipole factors for such systems and then apply them to our data.

**A. Equilibrium Behavior. 1. Isotropic Phase.** The static permittivity $\epsilon_{r0}$ is given by the relation[41,42]

$$\epsilon_{r0} - \epsilon_\infty = \frac{4\pi}{3kT} \frac{3\epsilon_{r0}(2\epsilon_{r0} + \epsilon_\infty)}{(2\epsilon_{r0} + 1)^2} \frac{\langle \mathbf{M}(0)\cdot\mathbf{M}(0)\rangle}{V} \quad (4)$$

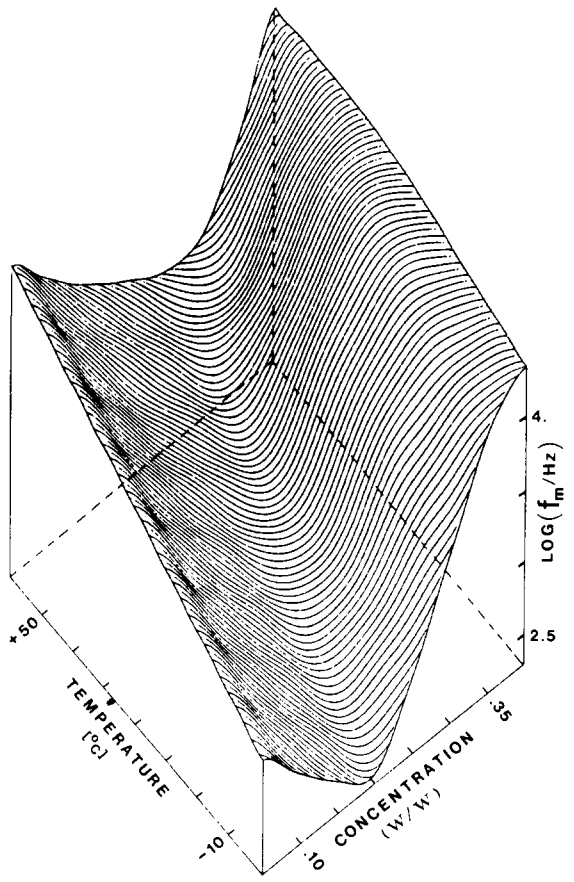


**Figure 10.** log ($f_m$/Hz) as a function of $c$ and $T$/°C for PHIC in toluene.

$\mathbf{M}(0)$ is the instantaneous dipole moment of a macroscopic sphere of volume $V$ and $\langle \mathbf{M}(0)\cdot\mathbf{M}(0)\rangle$ is its mean-square dipole moment, where the average is taken over all configurations of the ensemble in the sphere. For the PHIC–toluene isotropic solutions studied here, the solvent, which is only weakly dipolar, makes only a very small contribution to $\epsilon_{r0} - \epsilon_\infty$ so the magnitude of the relaxation is approximately represented by the contribution from the polymer chains, where

$$\langle \mathbf{M}(0)\cdot\mathbf{M}(0)\rangle_p = \langle \sum_i^N \mathbf{P}_i(0)\cdot\sum_i^N \mathbf{P}_i(0)\rangle = \sum_i^N\sum_i^N \langle \mathbf{P}_i(0)\cdot\mathbf{P}_i(0)\rangle = \sum_i \langle \mathbf{P}_i(0)\cdot\mathbf{P}_i(0)\rangle + \sum_i\sum_{i\neq i'} \langle \mathbf{P}_i(0)\cdot\mathbf{P}_{i'}(0)\rangle \quad (5)$$

$N$ is the total number of polymer chains, $\mathbf{P}_i(0)$ is the instantaneous dipole moment of molecule $i$, and $\langle \mathbf{P}_i(0)\cdot\mathbf{P}_i(0)\rangle \equiv \langle P_i^2\rangle = \langle P^2\rangle$ is its mean-square value. The terms $\langle \mathbf{P}_i(0)\cdot\mathbf{P}_{i'}(0)\rangle$ arise from angular correlations between different chains $i$ and $i'$ and may be important for concentrated solutions. For a monodisperse polymer in solution, eq 5 may be written as

$$\langle \mathbf{M}(0)\cdot\mathbf{M}(0)\rangle_p = N\langle P^2\rangle g_1 \quad (6)$$

where

$$g_1 = 1 + \frac{1}{N}\sum_i\sum_{i\neq i'} \frac{\langle \mathbf{P}_i(0)\cdot\mathbf{P}_{i'}(0)\rangle}{\langle P^2\rangle} = 1 + \sum_{i\neq l} \frac{\langle \mathbf{P}_l(0)\cdot\mathbf{P}_{i'}(0)\rangle}{\langle P^2\rangle} \quad (7)$$

Here we have used the equivalence of the chains, and $\langle \mathbf{P}_l(0)\cdot\mathbf{P}_{i'}(0)\rangle$ are terms expressing the angular correlation between a reference chain $l$ and a different chain $i'$. Now the "liquid" and "vacuum" dipole momemts, $\mathbf{P}_i$ and ${}^0\mathbf{P}_i$, may be related according to[41,42]

$$\mathbf{P}_i = {}^0\mathbf{P}_i \frac{(\epsilon_\infty + 2)(2\epsilon_{r0} + 1)}{3(2\epsilon_{r0} + \epsilon_\infty)} \quad (8)$$

From eq 4–8 we have

$$\epsilon_{r0} - \epsilon_\infty = \frac{4\pi}{3kT}\left[\frac{3\epsilon_{r0}}{2\epsilon_{r0} + \epsilon_\infty}\right]\left[\frac{\epsilon_\infty + 2}{3}\right]^2 c_p\langle {}^0P^2\rangle g_1 \quad (9)$$

where $c_p = N/V = N_A W_p/MV$ and $N_A$ is the Avogadro constant, $M$ is the molecular weight, and $W_p$ is the weight of the polymer in the volume $V$. In Figures 1–10 we have used $c$, defined as

$$c = 100 \times W_p/(W_p + W_s) \quad (10)$$

where $W_s$ is the weight of solvent in $V$. Assuming a simple mixing law for volumes, we have

$$\frac{W_p}{V} = \frac{W_p}{W_p\rho_p^{-1} + W_s\rho_s^{-1}} = 10^{-2}cF(\rho_p,\rho_s,c) \quad (11)$$

where

$$F(\rho_p,\rho_s,c) = \{1 + (\rho_p^{-1} - 1)10^{-2}c + (\rho_s^{-1} - 1)(1 - 10^{-2}c)\}^{-1} \quad (12)$$

and $\rho_p$ and $\rho_s$ are the densities of polymer and solvent, respectively. Thus eq 9 becomes

$$\epsilon_{r0} - \epsilon_\infty = \frac{4\pi N_A}{3kTM} f(\epsilon_{r0},\epsilon_\infty)F(\rho_p,\rho_s,c)10^{-2}c\langle {}^0P^2\rangle g_1 \quad (13)$$

where $f(\epsilon_{r0},\epsilon_\infty) = \{(\epsilon_\infty + 2)^2\epsilon_{r0}/3(2\epsilon_{r0} + \epsilon_\infty)\}$

For a polydisperse polymer whose distribution is characterized by the function $\zeta(M)$ we have

$$\langle \mathbf{M}(0)\cdot\mathbf{M}(0)\rangle_p = N\langle \bar{P}^2(M)\rangle \bar{g}_1 \quad (14)$$

where

$$\langle \bar{P}^2(M)\rangle = \sum_M \zeta(M)\langle P^2(M)\rangle / \sum_M \zeta(M) \quad (15a)$$

$$\bar{g}_1 = 1 + \sum_M \zeta(M)\sum_{j\neq l} \langle \mathbf{P}_{lM}(0)\cdot\mathbf{P}_{jM}(0)\rangle / \langle \bar{P}^2(M)\rangle + \sum_M \zeta(M)\sum_{M'}\sum_{j'} \langle \mathbf{P}_{lM}(0)\cdot\mathbf{P}_{j'M'}(0)\rangle / \langle \bar{P}^2(M)\rangle \quad (15b)$$

$\mathbf{P}_{lM}(0)$ is the instantaneous dipole moment of any given reference molecule $lM$ having a molecular weight $M$, $\mathbf{P}_{jM}$ is a similar quantity for a *different* molecule $jM$ having a molecular weight $M$, and $\mathbf{P}_{j'M'}$ is a similar quantity for a molecule $j'M'$ having molecular weight $M'$. Thus $\langle \bar{P}^2(M)\rangle$ is the mean-square dipole moment averaged over the distribution, and terms $\langle \mathbf{P}_{lM}(0)\cdot\mathbf{P}_{jM}(0)\rangle$ and $\langle \mathbf{P}_{lM}(0)\cdot\mathbf{P}_{j'M'}(0)\rangle$ are contributions arising from the correlations between a representative molecule $lM$ and molecules of the same molecular weight ($jM$) and of different molecular weight ($j'M'$), respectively. Now $\sum_M N(M) = (W_p/\bar{M}_n)N_A$, where $\bar{M}_n$ is the number-average molecular weight.[43] Thus eq 4, 5, 8, 14, and 15 give for a polydisperse isotropic solution

$$\epsilon_{r0} - \epsilon_\infty = \frac{4\pi N_A}{3kT\bar{M}_n} f(\epsilon_{r0},\epsilon_\infty)F(\rho_p,\rho_s,c)10^{-2}c\langle {}^0\bar{P}^2(M)\rangle \bar{g}_1 \quad (16)$$

Thus eq 16 shows that $\epsilon_{r0} - \epsilon_\infty$ is proportional to (i) $f(\epsilon_{r0},\epsilon_\infty)$, (ii) $F(\rho_p,\rho_s,c)10^{-2}c$, (iii) $\langle {}^0\bar{P}^2(M)\rangle$, and (iv) $\bar{g}_1$. As $c$ increases, $f(\epsilon_{r0},\epsilon_\infty)$ and $F(\rho_p,\rho_s,c)$ will vary in a calculable manner; thus $\langle {}^0\bar{P}^2(M)\rangle \bar{g}_1$ may be determined as a function of concentration.

**2. Lyotropic-Nematic Phase.** It is well-known from the work of Flory and co-workers (see, for example, ref 9–14 and references therein) that above a certain minimum

concentration, the material is biphasic, being an equilibrium mixture of the isotropic and "anisotropic" phases. Ignoring angular correlations between molecules in different phases, we write

$$\langle \mathbf{M}(0)\cdot\mathbf{M}(0)\rangle_p = {}_IN\sum_M({}_I\zeta(M))\langle {}_I\bar{P}^2(M)\rangle({}_I\bar{g}_1) + {}_AN\sum_M({}_A\zeta(M))\langle {}_A\bar{P}^2(M)\rangle({}_A\bar{g}_1) \quad (17)$$

where subscripts I and A refer to isotropic and anisotropic phases, respectively. Writing ${}_IN = \sum_M({}_IN(M)) = ({}_IW_p)N_A/({}_I\bar{M}_n)$ and with a similar relation for ${}_AN$, we obtain for the relaxation magnitude

$$\epsilon_{r0} - \epsilon_\infty = \Phi({}_I\Lambda) + (1-\Phi)({}_A\Lambda) \quad (18)$$

where

$${}_I\Lambda = \frac{4\pi N_A}{3kT}\frac{1}{({}_I\bar{M}_n)}\{{}_If(\epsilon_{r0},\epsilon_\infty)\}\{{}_IF(\rho_p,\rho_s,{}_Ic)10^{-2}({}_Ic)\}\langle {}_I{}^0\bar{P}^2(M)\rangle({}_I\bar{g}_1) \quad (19)$$

$${}_A\Lambda = \frac{4\pi N_A}{3kT}\frac{1}{({}_A\bar{M}_n)}\{{}_Af(\epsilon_{r0},\epsilon_\infty)\}\{{}_AF(\rho_p,\rho_s,{}_Ac)10^{-2}({}_Ac)\}\langle {}_A{}^0\bar{P}^2(M)\rangle({}_A\bar{g}_1) \quad (20)$$

and where $\Phi = {}_IV/({}_IV + {}_AV)$ is the volume fraction of the isotropic phase.

According to eq 18–20, the isotropic and anisotropic phases, having polymer concentrations of ${}_Ic$ and ${}_Ac$, respectively, and for which the distributions of molecular species, being ${}_I\zeta(M)$ and ${}_A\zeta(M)$, respectively, are different from the distribution for the unpartitioned system (see ref 9–14 and below), contribute strength factors ${}_I\Lambda$ and ${}_A\Lambda$ weighted by the volume fractions $\Phi$ and $1-\Phi$ of the two phases.

**3. Analysis of Data for $\epsilon_{r0}$.** Figure 4c shows $\epsilon_{r0}$ as a function of $c$ (percent (w/w)). For $0 < c < 15\%$, $\epsilon_{r0}$ is a linear function of $c$. In this range the solutions are optically isotropic and we may assert that they are isotropic in the sense that all molecules may, through Brownian motion, randomize their dipole vectors into a $4\pi$ solid angle. Equation 16 applies for such isotropic solutions, so it is of interest to obtain information on the concentration dependence of $\langle {}^0\bar{P}^2(M)\rangle\bar{g}_1$ in the range up to $c = 15\%$. We note that Coles and co-workers[33] have given data for $\epsilon_{r0} - \epsilon_\infty = \Delta\epsilon$ for PHIC–toluene solutions in the isotropic range. For $\bar{M}_w = 6.2 \times 10^4$, $\Delta\epsilon/c$ first increased and then decreased with increasing $c$ but for $\bar{M}_w$ equal to $1.4 \times 10^5$ and $2.9 \times 10^5$, $\Delta\epsilon/c$ showed a gradual decrease with increasing $c$ up to the maximum concentration of $c \simeq 1\%$ (w/w). From these and other dielectric and Kerr effect data they concluded that the chains tend to take up antiparallel arrangements with respect to the dipole vectors, leading to a decrease in $\bar{g}_1$ as $c$ is increased. Now $\langle {}^0\bar{P}^2\rangle\bar{g}_1$ is proportional to $(\Delta\epsilon/c)\{f(\epsilon_{r0},\epsilon_\infty)F(\rho_p,\rho_s,c)\}^{-1}$ (see eq 13). We note that Coles and co-workers have a different internal field factor (see their eq 1) but for both cases $\{f(\epsilon_{r0},\epsilon_\infty)\}^{-1}$ decreases with increasing $c$. $F(\rho_p,\rho_s,c)$ is approximately constant for $c < 1\%$ so $\langle {}^0\bar{P}^2\rangle\bar{g}_1$ decreases with increasing $c$. However, our data in Figure 4c give a linear relation of $\Delta\epsilon/c$ with $c$ for the range $5\% < c < 15\%$. For this range $\{f(\epsilon_{r0},\epsilon_\infty)\}^{-1}$ falls by 2% and $\{F(\rho_p,\rho_s,c)\}^{-1}$ falls by 1%, so multiplying the constant $\Delta\epsilon/c$ by $f^{-1}F^{-1}$ gives only a 3% decrease in $\langle {}^0\bar{P}^2\rangle\bar{g}_1$ in this range. Thus our data for PHIC (and PBNIC) give no evidence for the formation of antiparallel arrangements of chains for isotropic solutions in the range $5\% < c < 15\%$. For higher concentrations there is a distinct fall of $\epsilon_{r0}$ away from linear behavior with increasing $c$ for both PHIC and PBNIC. While this could be interpreted for isotropic solutions as being due to a fall in $\langle {}^0\bar{P}^2\rangle\bar{g}_1$, arising from antiparallel arrangements of chains, we do not think that this is the case. Rather, we consider the gradual fall, followed by the dramatic fall, in $\epsilon_{r0}$ to be due to the formation of the biphasic material, as expected from the works of Flory and Aharoni. It is therefore appropriate, at this point, to summarize the essential features of the phase behavior of an assembly of rods in solution as developed through the model calculations of Flory and co-workers.

Flory[9,10] showed, for a monodisperse system of rods in solution, that the system was isotropic up to a volume fraction of polymer $v_2{}^0{}^*$, beyond which it became "biphasic". The biphasic system was an equilibrium mixture of isotropic (I) and anisotropic (A) phases, where the latter phase corresponded to a lyotropic-nematic arrangement of the rods. In the biphasic range the volume fraction of I phase, $\Phi$ say, decreased monotonically with increasing volume fraction of polymer, $v_2{}^0$, to the point at which $\Phi \simeq 0$. For higher values of $v_2{}^0$ the system was essentially anisotropic phase. The initial theory of Flory was athermal, i.e., was based on configurational entropy only, but subsequently Flory[9,10] introduced interactions between the rods via a quantity $\chi$ which depended upon temperature. Flory and co-workers[11-14] extended the earlier work to include the effects of polydispersity. In particular, Flory and Frost[13,14] calculated the phase behavior for systems having the "most probable" and Poisson distributions of molecular length and showed, importantly, that partial fractionation of species occurs between the isotropic and anisotropic phases of the biphasic system, with the high molecular weight species favoring the anisotropic phase. Subsequently, Aharoni and Walsh[3,4] showed that PHIC and other poly(n-alkyl isocyanates) at high polymer concentrations in such solvents as toluene and trichloroethylene formed lyotropic media and, further, showed that in the biphasic range the two phases could be separated physically and they confirmed the partial fractionation predicted by Flory and co-workers.[9-14] The "most probable" and Poisson distribution functions are of fixed shape (e.g., half-width and its asymmetry) once the average chain-length has been specified. Therefore Moscicki and Williams[44,45] extended the calculations to the case of a Gaussian distribution whose width was variable for a given average chain length. The Gaussian distribution leads to the following relation for the volume fraction of $X$-meric species in the unseparated system, $v_X{}^0$:

$$\frac{v_X{}^0}{v_2{}^0} = \frac{X}{\bar{X}}\exp\left\{-(4\ln 2)\left[\frac{X - X_0}{\Delta_{1/2}}\right]^2\right\} \quad (21)$$

$X$ is the number of units in a chain, $\bar{X} = \sum Xn_X{}^0/n_2{}^0$, where $n_X{}^0$ is the total number of $X$-meric species in a sample volume $V$, $n_2{}^0$ is the total number of polymer (solute) species and is given by $n_2{}^0 = \sum n_X{}^0$. Also $v_X{}^0$ and $v_2{}^0$ are the volume fractions of $X$-meric species and all polymer species, respectively, in both phases combined.[11-14] $\Delta_{1/2}$ is the total half-width of the Gaussian curve and $X_0$ is the value of $X$ at the maximum of the Gaussian distribution. $v_2{}^0$ and polymer concentration $c$ (% (w/w)) are related according to

$$z = 100\left\{1 + \frac{\rho_s}{\rho_p}\left(\frac{1}{v_2{}^0} - 1\right)\right\}^{-1} \quad (22)$$

where for PHIC in solution in toluene $\rho_s = 0.866$ and $\rho_p = 1.00$ in units of g cm$^{-3}$. We have calculated $\Phi_A = 1 - \Phi$, being the volume fraction of anisotropic phase, for different

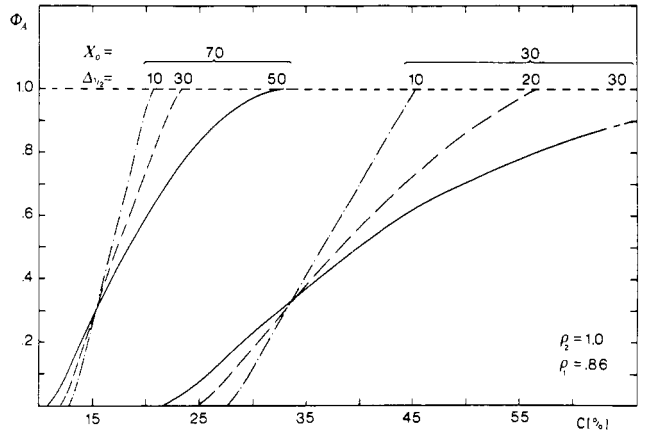


**Figure 11.** $\Phi_A$ against $c(\%)$ for $\rho_s = 0.866$, $\rho_p = 1.00$, and $X_0 = 70$ and 30 for different values of $\Delta_{1/2}$.

values of $X_0$, $\Delta_{1/2}$, and $c$ (% (w/w)). The values of $X_0$ ranged from 30 to 70 in steps of 10 and $\Delta_{1/2}$ values ranged from 10 to 50 in steps of 10.

Figure 11 shows plots of $\Phi_A$ against $c(\%)$ for $X_0$ equal to 30 and 70 and for different values of $\Delta_{1/2}$. Consider first the curve for $X_0 = 70$ and $\Delta_{1/2} = 10$. In the isotropic range $\Phi_A$ is, of course, zero. For $c > 12.7\%$ the biphasic system is formed, $\Phi_A$ increasing rapidly and reaching unity for $c \simeq 20.0\%$. For higher values of $c$ the system is essentially wholly anisotropic. Thus in the range $12.7\% < c < 20\%$ the biphasic system prevails. The effect of broadening the Gaussian curve for fixed average chain length is seen for the curves for $X_0 = 70$ and $\Delta_{1/2}$ equal to 10, 30, and 50. As $\Delta_{1/2}$ is increased, the critical concentration, $c^*$ say, for the formation of the biphasic system decreases from 12.7 to 12.0 to 11.0% for $\Delta_{1/2}$ increasing from 10 to 30 to 50, respectively. Also the range of concentration over which the biphasic system exists is greatly increased as $\Delta_{1/2}$ is increased. Reducing $X_0$ to 30 gives the curves shown in Figure 11 for $\Delta_{1/2}$ equal to 10, 20, and 30. $c^*$ is seen to increase as $X_0$ is decreased for given values of $\Delta_{1/2}$; i.e., if the average chain length is reduced, we must go to higher polymer concentration in order to form the biphasic system. Also a decrease in $X_0$ leads to an extension of the range of concentration for the existence of the biphasic system for given values of $\Delta_{1/2}$; i.e., the transformation from an isotropic to a wholly anisotropic system becomes more diffuse as average chain length is reduced. Note also that variation of $\Delta_{1/2}$ has a much greater effect on the curves for $X_0 = 30$ than those for $X_0 = 70$. Figure 12 shows, as examples, the variation of the volume fractions of polymer in the isotropic phase, $\upsilon_2$, and the anisotropic phase, $\upsilon_2'$, for $X_0 = 70$, $\Delta_{1/2} = 30$ and for $X_0 = 30$, $\Delta_{1/2} = 10$. $\upsilon_2$ and $\upsilon_2'$ obey the conservation relation

$$\upsilon_2^0 = \Phi\upsilon_2 + \Phi_A\upsilon_2' = (1 - \Phi_A)\upsilon_2 + \Phi_A\upsilon_2' \qquad (22a)$$

Consider the plots for $X_0 = 70$, $\Delta_{1/2} = 30$. As $c(\%)$ is increased in the isotropic range, $\upsilon_2 = \upsilon_2^0$.

At $c = c^*$ the biphasic system forms and the volume fraction of polymer in the isotropic phase, $\upsilon_2$, increases only slightly in the biphasic range $c^* < c < c^{**}$, where $c^{**}$ is the concentration at which the system becomes wholly anisotropic. For $X_0 = 70$, $\Delta_{1/2} = 30$, $c^* = 12.0\%$ and $c^{**} = 23.3\%$. At $c = c^* = 12.0\%$, $\upsilon_2 \simeq 0.108$ and $\upsilon_2'$, the volume fraction of polymer in the anisotropic phase, is about 0.181, giving a ratio $\upsilon_2'/\upsilon_2 = 1.6$, which changes only slightly as the biphasic range is traversed. A simple physical interpretation would be that when $c$ is raised to $c^*$, the isotropic solution becomes saturated with polymer so for $c > c^*$ the anisotropic phase, whose polymer concentration is about 50% higher than that for the isotropic phase, forms in increasing amount (measured by $\Phi_A$) until the system becomes wholly anisotropic at $c \rightarrow c^{**}$. For $c > c^{**}$, we have the relation $\upsilon_2' = \upsilon_2^0$ so there is a simple geometrical connection in the plots $\upsilon_2$, $\upsilon_2'$ against $\upsilon_2^0$ for the lines for the wholly isotropic phase (where $\upsilon_2 = \upsilon_2^0$) and for the wholly anisotropic phase (where $\upsilon_2' = \upsilon_2^0$). Also shown in Figure 12 are plots of $(1 - \Phi_A)\upsilon_2$ and $\Phi_A\upsilon_2'$ against $c$ in the biphasic range for $X_0 = 70$, $\Delta_{1/2} = 30$. These quantities are proportional to the number of polymer molecules in the isotropic and anisotropic phases, respectively, and so give a part of the information required for the calculation of the contributions from each phase to the total dielectric relaxation magnitude.

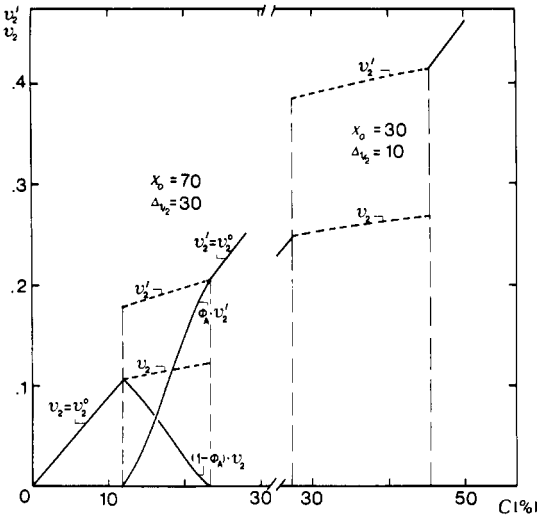


**Figure 12.** $\upsilon_2$, $\upsilon_2'$, $\Phi_A\upsilon_2'$, and $(1 - \Phi_A)\upsilon_2$ against $c(\%)$ for $X_0 = 70$, $\Delta_{1/2} = 30$ and for $X_0 = 30$, $\Delta_{1/2} = 10$, using $\rho_s = 0.866$ and $\rho_p = 1.00$ in units of g cm$^{-3}$.

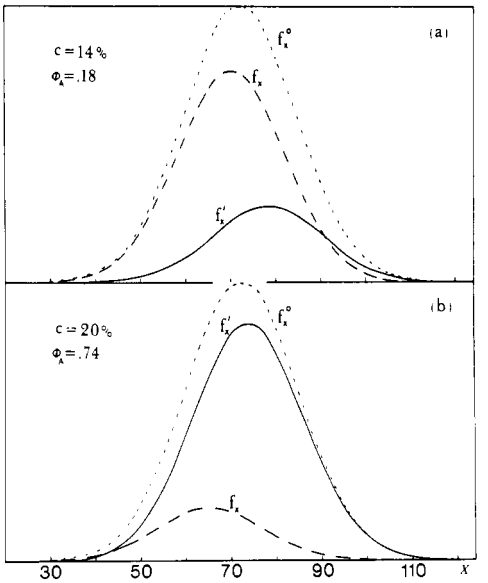


**Figure 13.** $f_X^0$, $f_X$, and $f_X'$ against $X$ for $X_0 = 70$ and $\Delta_{1/2} = 30$. Curves a and b refer to $c = 14\%$ and $c = 20\%$, respectively.

Accompanying the phase behavior indicated in Figures 11 and 12 is the partial fractionation of the system in the biphasic range. Figure 13 shows, as an example, plots of $f_X$ and $f_X'$ against $X$ for $X_0 = 70$, $\Delta_{1/2} = 30$ and for $c = 14\%$ and $c = 20\%$. Here $f_X$ and $f_X'$ are the amounts of $X$-mer in the isotropic and anisotropic phases, respectively, as defined by Flory and Frost.[12,13]

$$f_X = \Phi\upsilon_X/\upsilon_2^0 \qquad (23a)$$

$$f_X' = \Phi_A v_X'/v_2^0 \quad (23b)$$

where

$$f_X^0 = v_X^0/v_2^0 = f_X + f_X' \quad (24)$$

According to the results shown in Figure 13, for $c = 14\%$, the chains partition between the isotropic and anisotropic phases, with the longer chains favoring the anisotropic phase and the shorter chains the isotropic phase, when comparison is made with the parent function $f_X^0$. At this concentration the isotropic phase is predominant ($\Phi_A \simeq 0.18$ from Figure 11) as is evident from the relative magnitudes of $\sum f_X$ and $\sum f_X'$. For $c = 20\%$ we have a pattern of behavior similar to that for the lower concentration, only now the anisotropic phase is predominant ($\Phi_A \simeq 0.74$ from Figure 11). Thus the model calculations give us a physical insight into the formation of isotropic, biphasic, and anisotropic systems composed of rodlike molecules, they indicate the composition of the phases in the biphasic range (in terms of $v_2$, $v_2'$, $f_X$, $f_X'$), and they indicate the relative amounts of isotropic and anisotropic phases (in terms of $\Phi = 1 - \Phi_A$).

In considering the application of such calculations to our data, we must remember that they are derived for athermal solutions composed of rodlike particles and solvent particles. Clearly, temperature plays an important role in determining the phase behavior of PHIC–toluene solutions (see Figures 3 and 6–9). As $T$ is lowered, $c^*$ decreases and this gives the marked decrease in $\epsilon''_m$ seen in Figures 6–8 and the variation in the locus of the maximum in $\epsilon''_m(T,c)$ seen in Figure 9. Thus intermolecular interactions, which are absent in the "athermal" calculations, do play an important part in determining the phase behavior of PHIC solutions. Also we have to ask if PHIC is rodlike in solution. There seems little doubt that such molecules are rodlike for $M < 10^4$, in view of the large persistence length,[31,39] but at higher molecular weight there is a tendency for the chains to form broken rods or wormlike chains.[27,28,31,32] Evidence is provided by dielectric and Kerr effect data for poly(*n*-butyl isocyanate) and poly(*n*-octyl isocyanate), where it was found[32,33] that $T\Delta\epsilon$ decreases by about 20% in a range of 30 K due to a fall in $\langle {}^0\bar{P}^2\rangle\bar{g}_1$, and the static Kerr constant decreased[33] by 50% in a range of 30 K due to decreases in $\langle {}^0\bar{P}^2\rangle\bar{g}_1$ and the anisotropy of optical polarizability $\Delta\alpha(M)$. However, PHIC is rodlike for long sequences of the chain and does form liquid-crystal mesophases; therefore it is of interest to see if our dielectric data may be interpreted to some extent in terms of the Flory theory, as considered by us for a Gaussian distribution.

From Figure 4c it appears that significant departures from isotropic-phase behavior occur for $c > 15\%$ for both PHIC and PBNIC. For the range $15\% < c < 21\%$, $\epsilon_{r0}$ falls below the linear relation but for $22\% < c < 35\%$ there is a dramatic change in behavior. For $c > 35\%$ the material is essentially anisotropic. According to eq 13, $\Delta\epsilon$(isotropic) will be approximately proportional to $c$ if $\langle {}^0\bar{P}^2(M)\rangle\bar{g}_1$ is constant. In eq 18, $\Delta\epsilon$(biphasic) will be due to the sum of contributions from the two phases as indicated. Now ${}_Ic$ and ${}_Ac$ will be, respectively, proportional to $\Phi v_2$ and $(1 - \Phi)v_2'$. The factors $\langle {}_I{}^0\bar{P}^2(M)\rangle({}_I\bar{g}_1)$ and $\langle {}_A{}^0\bar{P}^2(M)\rangle({}_A\bar{g}_1)$ are very different. The first factor will be similar to that obtained for the wholly isotropic phase, with the important difference that the partial fractionation (see Figure 13) enriches the isotropic phase in the biphasic material with low molecular weight species. The second factor, $\langle {}_A{}^0\bar{P}^2(M)\rangle({}_A\bar{g}_1)$, is influenced by the partial fractionation of high molecular weight species into the anisotropic phase, but its value will be less than $\langle {}_I{}^0\bar{P}^2(M)\rangle({}_I\bar{g}_1)$ because in the anisotropic phase the dipole vectors are unable to reorientate into a $4\pi$ solid angle but will be restricted to a virtual cone. This means that only a portion of $\langle {}^0\bar{P}^2(M)\rangle$ can be relaxed; thus $\Delta\epsilon$(anisotropic) < $\Delta\epsilon$(isotropic) when compared at the same overall concentration (via extrapolation of the data for the isotropic liquid).

According to Figure 13, $\Delta\epsilon$(isotropic) will increase linearly with $c$ up to $c = c^*$, after which $\Delta\epsilon$(biphasic) is a weighted sum of terms proportional to $\{(1 - \Phi_A)v_2\langle {}_I{}^0\bar{P}^2(M)\rangle({}_I\bar{g}_1)\}$ and $\{\Phi_A v_2'\langle {}_A{}^0\bar{P}^2(M)\{({}_A\bar{g}_1)\}$. This immediately implies that $\Delta\epsilon$ reaches a maximum value at $c = c^*$ and then decreases to the point $c = c$(biphasic → anisotropic), after which it again increases due to the increase in $v_2$. Our experimental data show a fall away of $\epsilon_{r0}$ from linearity before the peak is reached, and this cannot be explained by the model theory, even allowing for the complications of partial fractionation. We are thus led to speculate that if the athermal theory is extended to include temperature-dependent molecular interactions, a sharp break in $v_2$ at $c = c^*$ would not be expected but instead a gradual rounding-off of the curve would occur so that $v_2$ would fall below linear behavior around the $c = c^*$ condition. This would also imply that $v_2'$ does not "step on" but follows a curve ranging from zero up to the curve for the biphasic range. In other words, it may be that the inclusion of molecular interactions will make the calculated transition from isotropic to biphasic material a little more diffuse.

Consider now the range $21\% < c < 35\%$. In this range $\Delta\epsilon$ falls remarkably and is to be interpreted as being primarily due to a fall in $(1 - \Phi_A)v_2\langle {}_I{}^0\bar{P}^2(M)\rangle({}_I\bar{g}_1)$ as $c$ is increased. While this term falls rapidly via $(1 - \Phi_A)v_2$ as indicated in Figure 12, there will also be a fall in $\langle {}_I{}^0\bar{P}^2(M)\rangle({}_I\bar{g}_1)$ due to the partial fractionation which places the lower molecular weight species, on the average, into the isotropic phase. The mean-square dipole moment of PHIC decreases rapidly with decreasing molecular weight[27,28,31,33] so $\langle {}_I{}^0\bar{P}^2(M)\rangle({}_I\bar{g}_1)$ is expected to fall over that obtainable for the wholly isotropic phase at $c < c^*$. A detailed numerical analysis of $\Delta\epsilon$ for the biphasic range will not be attempted in this paper.

At the highest concentrations and lowest temperatures the composition of the material approaches that of the anisotropic phase. From Figure 4c we obtain $G = \Delta\epsilon$(anisotropic)/$\Delta\epsilon$(isotropic) $\simeq 0.07$ for $c = 40\%$, where $\Delta\epsilon$(isotropic) is obtained by linear extrapolation of the isotropic data. As mentioned above, $G \ll 1$ since the chains may only undergo limited angular motion in the anisotropic phase. If a rodlike chain is constrained to move in a cone, then the magnitude of the loss process is proportional to $\{\langle\mu^2\rangle - \langle\mu\rangle^2\} = \langle\mu^2\rangle G$, where $\langle\mu^2\rangle$ is the mean-square dipole moment of the chain and $\langle\mu\rangle$ is the mean dipole moment residing in the cone after partial randomization of the dipole vector. Assuming the vector is free to move in the range $0 \le \theta \le \theta_0$, where $\theta$ is the polar angle for reorientation, but is not allowed outside this range leads to the result[36]

$$\cos\theta_0 = 2\{1 - G\}^{1/2} - 1 \quad (25)$$

Hence, using $G = 0.07$, we calculate $\theta_0 = 22°$. This is only a rough estimate since we have not taken into account the important effects of a molecular weight distribution and the dependence of dipole moment upon chain length. This value of $\theta_0$ gives us, however, an indication of the extent of motion which is allowed in the anisotropic phase and this will be considered further below.

**4. Analysis of Data for $\epsilon_r$.** The qualitative features of Figures 3–10 have already been discussed above. We note that in the isotropic range of the data in Figures 3 and 4 log $f_m$ decreases with increasing $c$, being due to the

increase in the macroscopic viscosity of the solutions, which increasingly hinders the motions of the chains. The shape of the loss curves and their overall half-width ($\Delta \log f \simeq 2.7$) vary only slightly with concentration. The interpretations of such loss curves for isotropic solutions have been given previously[27-33] and will not be further discussed here. From our account in A.3 above, it is evident that for Figures 6–8 our data refer to the biphasic and anisotropic phases, whose behaviors are qualitatively different. For Figures 7 and 8 with $T$ in the range 272–292 K the data appear to represent motion in the anisotropic phase. For Figure 6 at all temperatures studied and for Figures 7 and 8 at higher temperatures, the loss curves contain a substantial contribution from the isotropic phase; i.e., the material is biphasic in those ranges. For the anisotropic range $\epsilon''_m$ and log $f_m$ increase slightly with increasing temperature, corresponding to an increase in the extent of angular motion and its rate. According to the model of Warchol and Vaughan[37] and Wang and Pecora[38] for the small-step rotational diffusion of a rod in a cone, which we have previously considered for PBNIC–toluene solutions,[36] the dipole moment vector correlation function $\langle \mu(0)\cdot\mu(t)\rangle$ will be given by

$$\langle \mu(0)\cdot\mu(t)\rangle = \mu^2\{D_1^0 + D_2^0 \exp\{-\nu_2^0(\nu_2^0 + 1)D_R t\} + D_1^1 \exp\{-\nu_1^1(\nu_1^1 + 1)D_R t\}\} \quad (26)$$

$D_R$ is the rotational diffusion coefficient and $D_1^0 = \{(1 + \cos\theta_0)/2\}^2 = \{\langle\mu\rangle\}^2/\langle\mu^2\rangle$ and represents that part of $\langle\mu^2\rangle$ which may not be relaxed by motion in the cone (see eq 25). $D_2^0 = \{1 - \cos\theta_0\}^2/12$ and $D_1^1 = \{2 - \cos\theta_0 - \cos^2\theta_0\}/3$. For $\theta_0 < 60°$, $D_2^0$ is small in comparison with $D_1^0$ so $\langle\mu(0)\cdot\mu(t)\rangle$ for the rod would be characterized by a single-exponential decay with relaxation time $\tau_{\nu_1^1} = \{\nu_1^1(\nu_1^1 + 1)D_R\}^{-1}$ to a constant (plateau) value $D_1^0$. Thus only $D_2^0 + D_1^1 = 1 - D_1^0$ would be relaxed by motion in the cone. Wang and Pecora[38] give curves of $\nu_n^m(\theta_0)$ and it is found that $\nu_1^1(\theta_0)$ increases rapidly with decreasing $\theta_0$ for $\theta_0 < 30°$. For $\theta_0 = 22°$, which is the value calculated in section A.3 above, we have $\nu_1^1(30°) = 4.5\nu_1^1(180°)$. Thus $\tau_{\nu_1^1(30°)}$ will be ~20 times smaller for motion in the cone compared with that for motion into a $4\pi$ solid angle if $D_R$ remains constant. Inspection of Figure 4 shows that $\log f_m = -\log 2\pi\langle\tau\rangle$ does increase on going from isotropic, through biphasic, to the anisotropic phase but the increase is ~1.9 over that extrapolated from the isotropic phase, leading to $\tau$(anisotropic) being about 80 times smaller than that in the isotropic phase *extrapolated* to the common concentration. Such a calculation is only approximate since we have not considered the effect of a molecular weight distribution or the variation of $D_R$ with composition. This simple calculation does, however, rationalize the decrease in $\Delta\epsilon$ and $\langle\tau\rangle$ on going from an isotropic to an anisotropic phase in terms of the motions of chains restricted to a virtual cone in the anisotropic phase. With regard to the biphasic range, the overall loss curves (e.g., Figures 3 and 6) are a weighted sum of contributions from isotropic and anisotropic phases. The motions in the isotropic phase are slower, on the average, than those in the anisotropic phase at a given concentration so raising the temperature, which increases $\Phi v_2$, increases the magnitude of the loss process, and the overall loss peak moves to lower frequencies. Such behavior is observed in Figures 7 and 8 and yields a *negative* apparent activation energy for the overall process: The data of Figure 6 are especially interesting. As $T$ is increased in the range 253–292 K, $\epsilon''_m$ (and thus $\Delta\epsilon$) increases markedly and log $f_m$ increases slightly. On going from 292 to 313 K, $\epsilon''_m$ goes over a peak value and log $f_m$ increases more noticeably. The interpretation is that in the range 253–292 K the number of molecules in the isotropic phase ($\propto \Phi v_2$) increases markedly, with a corresponding decrease in the number of molecules in the anisotropic phase ($\propto (1 - \Phi)v_2'$), giving an overall increase in $\epsilon''_m$. The slight shift to higher frequencies is the result of superposing weighted contributions from isotropic and anisotropic phases and is not easily interpreted without going into detailed calculation. At the higher temperatures, 292–313 K, the material becomes wholly isotropic and now we see a decrease in $\epsilon''_m$ and an increase in log $f_m$ as is observed for dilute isotropic solutions—as discussed in section A.3—the decrease in $\epsilon''_m$ being due to the deviation of the chains from rigid-rod behavior.

The detailed analysis of the data of Figures 3 and 6–8 for the biphasic range and the anisotropic range involves the generalization of eq 13 and 18 to the dynamic situation. For the isotropic solutions we have, following Cook et al.[41]

$$\left[\frac{\epsilon_r - \epsilon_\infty}{\epsilon_{r0} - \epsilon_\infty}\right] p(\omega) = \mathcal{F}\left[\frac{-d\Gamma(t)}{dt}\right] \quad (27)$$

where

$$\Gamma(t) = \langle \mathbf{M}(0)\cdot\mathbf{M}(t)\rangle_p / \langle \mathbf{M}(0)\cdot\mathbf{M}(0)\rangle_p = \{\sum_M \zeta(M)\langle \mathbf{P}_{lM}(0)\cdot\mathbf{P}_{lM}(t)\rangle + \sum_M \zeta(M)\sum_{\substack{j \\ j\neq l}} \langle \mathbf{P}_{lM}(0)\cdot\mathbf{P}_{jM}(t)\rangle + \sum_M \zeta(M)\sum_{M'}\sum_{j'} \langle \mathbf{P}_{lM}(0)\cdot\mathbf{P}_{j'M'}(t)\rangle\} \times \{\langle \bar{\mathbf{P}}^2(M)\rangle \bar{g}_1\}^{-1} \quad (28)$$

and $p(\omega)$ is an internal field factor.[41] Equation 27 indicates that the one-sided Fourier transformation of the first time derivative of the normalized total dipole moment correlation function $\Gamma(t)$ gives the normalized complex permittivity. $\Gamma(t)$ is a weighted sum of auto- and cross-correlation terms and involves the distribution of molecular weight. For the isotropic solutions of PHIC it appears from our earlier discussion that the cross-correlation terms have a small magnitude in relation to the autocorrelation terms so the data for these solutions give information on $\sum_M \zeta(M)\langle \mathbf{P}_{lM}(0)\cdot\mathbf{P}_{lM}(t)\rangle$. Since $\langle \bar{P}^2(M)\rangle$ and $\tau(M)$ increase with molecular weight,[27-32] it follows that our data for the isotropic solutions are strongly influenced by the high molecular weight species in the distribution. For the biphasic material, eq 17 and 18 generalize to the following relation:

$$\frac{\epsilon_r - \epsilon_\infty}{\epsilon_{r0} - \epsilon_\infty} = \frac{\Phi({}_I\Lambda)}{\Phi({}_I\Lambda) + (1 - \Phi)({}_A\Lambda)} \mathcal{F}\{-d\Gamma_I(t)/dt\} + \frac{(1 - \Phi)({}_A\Lambda)}{\Phi({}_I\Lambda) + (1 - \Phi)({}_A\Lambda)} \mathcal{F}\{-d\Gamma_A(t)/dt\} \quad (29)$$

$\Gamma_I(t)$ and $\Gamma_A(t)$ are the normalized correlation functions for the isotropic and anisotropic phases in the biphasic material. They are defined in equations similar to eq 28 and we write

$$\Gamma_\alpha(t) = \{\sum_M ({}_\alpha\zeta(M))\langle \mathbf{P}_{lM}(0)\cdot\mathbf{P}_{lM}(t)\rangle_\alpha + \sum_M ({}_\alpha\zeta(M))\sum_{\substack{j \\ j\neq l}} \langle \mathbf{P}_{lM}(0)\cdot\mathbf{P}_{jM}(t)\rangle_\alpha + \sum_M ({}_\alpha\zeta(M))\sum_{M'}\sum_{j'} \langle \mathbf{P}_{lM}(0)\cdot\mathbf{P}_{j'M'}(t)\rangle_\alpha\}\{\langle {}_\alpha\bar{P}^2(M)\rangle ({}_\alpha\bar{g}_1)\}^{-1} \quad (30)$$

where $\alpha$ is "$I$" or "A" and the correlation functions refer to species of given molecular weight in a given phase.

Equations 29 and 30 show that the total loss curves in the biphasic range are a weighted sum of contributions from the two phases and, since the phases are in equilibrium, any change in the amount and composition of one phase brought about by variation of concentration and/or temperature will bring about corresponding changes in the

other phase. Thus the magnitude and location of the overall process in the biphasic range, as observed in Figures 6–8 result from the changes in composition, as judged by $\Phi v_2$ and $(1 - \Phi)v_2'$ and by the relative partitioning of species of different molecular weight between the phases (see Figure 13). It is our intention to model the loss curves for the biphasic and anisotropic ranges by using eq 28 and 29 and the results of calculations with the Flory theory, as presented here in Figures 11–13. For the present we note that for the data of Figure 6, the loss curves are mainly arising from the isotropic material while in Figures 7 and 8 they are mainly from the anisotropic material (with the exception of Figure 8, $T = 333.2$ K). In Figure 6, raising the temperature provides more isotropic material, via an increase in $\Phi v_2$, and there is a balance between log $f_m$ increasing with $T$ due to viscosity variation and log $f_m$ decreasing due to more isotropic material with higher molecular weight components being provided from the anisotropic phase. The result is that log $f_m$ is hardly changed in the range 250–293 K for $c = 25\%$. At higher concentrations, Figures 7 and 8 show that an increase in temperature creates more isotropic phase in materials that are initially predominantly anisotropic phase, and since the isotropic material relaxes far more slowly than the anisotropic material, there is a pronounced shift of log $f_m$ to lower values, giving an apparent activation energy of *negative* sign.

## Conclusions

It has been shown that dielectric measurements provide a useful means of studying the structure and dynamics of poly(*n*-hexyl isocyanate) in solution in the isotropic, biphasic, and anisotropic phases. These data provide support for the earlier observations of Aharoni and co-workers, using microscopy and viscosity techniques, for such rodlike polymers in solution. The dielectric studies have shown that the transformations isotropic → biphasic → anisotropic phase lead to a successive reduction of relaxation magnitude, $\Delta\epsilon$, and average relaxation time, $\langle\tau\rangle = \{2\pi f_m\}^{-1}$ and that the relaxation process in the anisotropic phase is far broader, and faster, than that for the isotropic phase. The phase transformations and the motions in the phases are found to be strongly dependent upon temperature, and the behavior may be rationalized, in a semiquantitative manner, with the aid of the Flory theory for concentrated polymer solutions and the theories of Warchol and Vaughan and of Wang and Pecora for limited angular diffusion of rods within a virtual cone prescribed by the neighboring molecules in the anisotropic phase.

**Acknowledgment.** We thank the S.R.C. for their continued support and for a Research Grant to J.K.M.

## References and Notes

(1) Aharoni, S. M. *Macromolecules* **1979**, *12*, 94.
(2) Aharoni, S. M.; Walsh, E. K. *J. Polym. Sci., Polym. Lett. Ed.* **1979**, *17*, 321.
(3) Aharoni, S. M.; Walsh, E. K. *Macromolecules* **1979**, *12*, 271.
(4) Aharoni, S. M. *Polymer* **1980**, *21*, 21.
(5) Aharoni, S. M. *Ferroelectrics* **1980**, *30*, 227.
(6) Aharoni, S. M.; Sibilia, J. P. 20th Canadian High Polymer Forum, Aug 1979.
(7) (a) Aharoni, S. M. *J. Polym. Sci., Polym. Phys. Ed.* **1980**, *18*, 1308. (b) *Ibid.* **1980**, *18*, 1439.
(8) Aharoni, S. M. *Polym. Prepr., Am. Chem. Soc., Div. Polym. Chem.* **1980**, *21* (1), 209.
(9) Flory, P. J. *Proc. R. Soc. London, Ser. A* **1956**, *234*, 73.
(10) Flory, P. J. *Ber. Bunsenges. Phys. Chem.* **1977**, *81*, 885.
(11) Flory, P. J.; Abe, A. *Macromolecules* **1978**, *11*, 1119.
(12) Abe, A.; Flory, P. J. *Macromolecules* **1978**, *11*, 1122.
(13) Flory, P. J.; Frost, R. S. *Macromolecules* **1978**, *11*, 1126.
(14) Frost, R. S.; Flory, P. J. *Macromolecules* **1978**, *11*, 1134.
(15) Robinson, C. *Trans. Faraday Soc.* **1956**, *52*, 571.
(16) Robinson, C.; Ward, J. C.; Beevers, R. B. *Discuss. Faraday Soc.* **1958**, *25*, 29.
(17) Hermans, J. *J. Colloid Sci.* **1962**, *17*, 638.
(18) Wee, E. L.; Miller, W. G. *J. Phys. Chem.* **1971**, *75*, 1446.
(19) Miller, W. G.; Rai, J. H.; Wee, E. L. In "Liquid Crystals and Ordered Fluids"; Johnson, J. F., Porter, R. S., Eds.; Plenum Press: New York, 1974; Vol. 2, p 243.
(20) Nakajima, A.; Hayashi, T.; Ohmori, M. *Biopolymers* **1968**, *6*, 973.
(21) Papkov, S. P. *Khim. Volokna* **1973**, *15*, 3.
(22) Papkov, S. P.; Kulichikhin, G.; Kalmykova, V. D. *J. Polym. Sci., Polym. Phys. Ed.* **1974**, *12*, 1753.
(23) Morgan, P. W. *Polym. Prepr., Am. Chem. Soc., Div. Polym. Chem.* **1976**, *17*, 47.
(24) Kwolek, S. L.; Morgan, P. W.; Schaefgen, J. R.; Gulrich, L. W. *Polym. Prepr., Am. Chem. Soc., Div. Polym. Chem.* **1976**, *17*, 53.
(25) Williams, G. *Chem. Rev.* **1972**, *72*, 55.
(26) Williams, G. *Chem. Soc. Rev.* **1978**, *7*, 89.
(27) Yu, H.; Bur, A. J.; Fetters, L. *J. Chem. Phys.* **1966**, *44*, 2568.
(28) Bur, A. J.; Roberts, D. E. *J. Chem. Phys.* **1969**, *51*, 406.
(29) Dev, S. B.; Lochhead, R. Y.; North, A. M. *Discuss. Faraday Soc.* **1970**, *49*, 244.
(30) Pierre, J.; Marchal, E. *J. Polym. Sci., Polym. Lett. Ed.* **1975**, *13*, 11.
(31) Bur, A. J.; Fetters, L. *Chem. Rev.* **1976**, *76*, 727.
(32) Beevers, M. S.; Garrington, D. C.; Williams, G. *Polymer* **1977**, *18*, 540.
(33) Coles, H. J.; Gupta, A. K.; Marchal, E. *Macromolecules* **1977**, *10*, 182.
(34) Jennings, B. R.; Brown, B. L. *Eur. Polym. J.* **1971**, *7*, 805.
(35) Moscicki, J. K.; Williams, G.; Aharoni, S. M. *Polymer* **1981**, *22*, 571.
(36) Moscicki, J. K.; Aharoni, S. M.; Williams, G. *Polymer* **1981**, *22*, 1361.
(37) Warchol, M. P.; Vaughan, W. E. *Adv. Mol. Relaxation Processes* **1978**, *13*, 317.
(38) Wang, C. C.; Pecora, R. *J. Chem. Phys.* **1980**, *72*, 5333.
(39) Berger, M. N.; Tidswell, B. M. *J. Polym. Sci., Polym. Symp.* **1973**, *42*, 1063.
(40) See, for example: Druon, C.; Warenier, J. M. *J. Phys. (Paris)* **1977**, *38*, 47.
(41) Cook, M.; Watts, D. C.; Williams, G. *Trans. Faraday Soc.* **1970**, *66*, 2503.
(42) Fröhlich, H. "Theory of Dielectrics"; Oxford University Press: London, 1958; p 181.
(43) See: Billmeyer, F. W. "Textbook of Polymer Science", 2nd ed.; Wiley-Interscience: New York, 1971; p 65.
(44) Moscicki, J. K.; Williams, G. *Polymer* **1981**, *22*, 1451.
(45) Moscicki, J. K.; Williams, G. *Polymer*, in press.
(46) This would give a negative apparent activation energy since $Q_{app} = -R(\delta \ln f_m/\delta T^{-1})$.